EXPERIMENTAL INVESTIGATION OF PROCESS PARAMETERS ON 64 SLICE SPIRAL CT SCANNER OF MEDICAL MODELS

Y. Ravi Kumar, A. Manmadhachary and L. Krishnanand

Department of Mechanical Engineering, National Institute of Technology Warangal, Telangana, 506004, India.

REVIEWED

Abstract

Rapid Prototyping (RP) is one of the advanced manufacturing methods to develop medical models. These models are generated by 3-Dimensional (3D) Computer Aided Design (CAD) model using Computed Tomography (CT) images. One of the advanced CT scanners to capture the large volume of tissues in shorter scan time is 64 slice spiral CT scanner. While developing these medical models, dimensional and volumetric errors occur due to Beam Hardening (BH) effect. This work has led to explore the influence of various CT Image acquisition parameters on the dimensional and volumetric errors, which are evaluated experimentally. A L_9 orthogonal array and signal to noise ratio are applied to study performance characteristics of CT image acquisition parameters like tube voltage, tube current and pitch. The experimental results are analyzed by using the analysis of variance (ANOVA) method and significant factors are identified. In this work, it has been concluded that there is a reduction of dimensional error from 1.43 mm to 0.52 mm and volumetric error from 6793 mm^3 to 3892 mm^3.

Key words: CT, Dimensional error, Volumetric error, Rapid prototyping, CT image acquisition, ANOVA.

Introduction

Rapid Prototyping (RP) is the automatic construction of physical objects using solid freeform fabrication. In other words, RP is an additive fabrication process refers to a group of technologies used for building physical models, prototypes, tooling components, finished series production parts all from 3-Dimensional (3D) Computer Aided Design (CAD) data, Computed Tomography (CT) or Magnetic Resonance Imaging (MRI) scans, or data from 3D scanning systems [1]. Unlike machining processes, which are subtractive in nature, RP's additive systems join together liquid, powder, or sheet materials to form parts [2]. Parts that may be difficult or even impossible to manufacture by any other method can be produced by additive systems [3]. Based on thin, horizontal cross sections taken from a 3D computer model, they produce plastic, metal, ceramic, or composite parts, layer upon layer.

Most of these RP systems generally adopt the standard processing steps to produce a part. They are created from 3D CAD modelling of the part to be produced, convert the CAD files into a RP industrial standard data file format, import the data file into the RP program of that system, check for errors and missing data in the data file, perform corrections where necessary, digitally slice the 3D CAD solid model into horizontal layers, send the sliced data to the RP machine for production and post-process the prototype such as removing redundant materials [2].

RP is one of the advanced manufacturing techniques to produce 3D physical medical models. These medical models are widely used for several applications like visualization,

diagnosis, surgery planning [4], design of implants, external prosthesis, surgical templates, production of artificial organs, communication between the medical team and/or medical doctors and patients, and teaching aids [5]. In the present work, CT images are considered as input data to produce 3D physical medical models. During acquisition of the CT images from the human anatomy, usually various dimensional and volumetric errors occur due to Beam Hardening (BH) effect [6].The presence of dense material in the middle portion of a uniform cylindrical phantom influences the X-rays in becoming hard as compared to the rays passing through the edges, which has shown in Fig.1. The hardened beam has less attenuation and intense as it reaches the detector; therefore, the difference in the attenuation profiles of this from that of ideal with beam hardening artifact. This artifact is also called "cupping" artifact because the hardening is more in the center and less on the periphery, it resembles a cup, which has shown in Fig. 1.

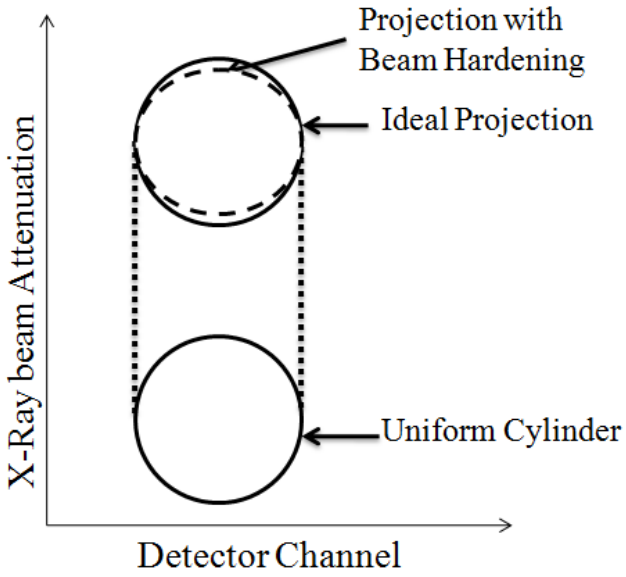

Fig. 1: BH effect on cylindrical phantom

Dual energy CT systems scan at two energy levels, which enable BH correction [7]. In dual energy CT systems, the X-ray beam energy is half the single X-ray CT scan systems so as to reduce the radiation dosage to the patient [8]. But this lower energy X-ray beam gives raise to image noise (photon starvation). So instead of dual energy CT scanner, single X-ray beam CT scanners are being used by manipulating tube voltage, tube current and pitch. To overcome BH effect, increasing in tube voltage [9] and tube current [10] ultimately increases the X-ray beam energy. Selections of optimum scanner parameters like tube voltage, tube current and pitch are the very important factors in avoiding dimensional and volumetric errors. Manufacturers and many authors are trying to eliminate the dimensional and volumetric errors using different cylindrical phantoms in a range of different sizes [11], but patient anatomy never exactly matches these cylindrical phantoms. X-ray beam photon attenuation is proportional to the density of the phantom [12]. In clinical practice generally bone is a phantom, but acrylic type of materials is used in experimental analysis. The acrylic materials and bone having different densities and Hounsfield Unit (HU) [11] values, due to this reason the variation will be observed in practice. In this study, a human dry mandible has been considered as a phantom for experimentation.

Experimental Setup

An adult dry mandible (Fig. 2) as a phantom for CT image acquisitions was used in this study to find dimensional and volumetric errors. This dry mandible has 110 mm length (X-axis), 80 mm width (Y-axis) and 65 mm height (Z-axis).

Fig. 2: Dry mandible phantom

The phantom was scanned with a 64 slice spiral CT scanner (Light Speed VCT, GE Medical Systems). The primary scan was done with default setting parameters of tube voltage 120 kV, tube current 300 mA and pitch 0.516 [13]. However, the other scans were done with different tube voltages, tube currents and pitches (shown in the Table 1) using L_9 orthogonal array. Further, optimized parameters produced were used for the last scan is a conformation test.

Table 1 CT Scanner acquisition parameters

Parameter	Level of Parameter		
	1	2	3
Tube voltage (kV)	120	100	80
Tube current (mA)	300	400	500
Pitch (table movement/slice thickness)	0.516	0.984	1.375

Scanning of the phantom with three different parameters (tube voltage, tube current and pitch) having three levels requires 3^3 (27) experiments. Taguchi method [15] uses a special design of orthogonal array to conduct the experiments and gives the optimize parameters. The degrees of freedom for three parameters in each of three levels were calculated by following equation.

Degree of Freedom (DOF) = number of levels -1---------- (1)

In this study three parameters and three levels were considered. So here L_9 standard orthogonal array is selected. This L_9 orthogonal array has eight DOF, in which 6 were assigned to three factors (each one 2 DOF) and 2 DOF was assigned to the error. Based on this L_9 orthogonal array (shown in the Table 2) nine scans were done with different tube voltage, tube current and pitch. The images in Digital Imaging and Communication in Medicine (DICOM) file format is used for developing 3D CAD model by utilizing Materialize Interactive Medical Image Control System (MIMICS) software (version 14.12, Materialise NV, Leuven, Belgium) [14].

Table 2 L_9 orthogonal array for experimentation

S.No	Experiment Number	Tube Voltage (kV)	Tube Current (mA)	Pitch
1	Exp. No. 1	120	300	0.516
2	Exp. No. 2	120	400	0.984
3	Exp. No. 3	120	500	1.375
4	Exp. No. 4	100	300	0.984
5	Exp. No. 5	100	400	1.375
6	Exp. No. 6	100	500	0.516
7	Exp. No. 7	80	300	1.375
8	Exp. No. 8	80	400	0.516
9	Exp. No. 9	80	500	0.984

To find the dimensional error, two X-axis (Fig. 3a), two Y-axis (Fig. 3b) and two Z-axis (Fig. 3c) dimensions were selected for measurement of the linear dimensions. These axes were similar to the CT scan machine axes (X, Y, and Z). The details of measurements of linear dimensions are shown in Appendix. In this paper the difference between dry mandible linear dimensions to the 3D CAD mandible linear dimensions values are considered as a dimensional error. This can be written as the following mathematical relations:

Dimensional error = Dry mandible dimension - 3D CAD mandible dimension---------- (2)

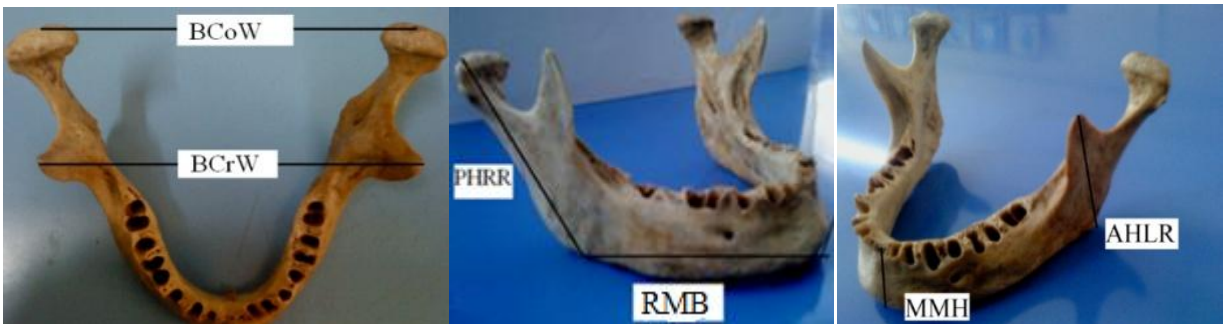

(a) (b) (c)

Fig. 3: Anatomic landmarks for measurements in (a) X-axis,(b) Y-axis and (c) Z-axis

The 3D CAD mandible linear dimensions (Fig. 4a) are measured using MIMICS software whereas a digital electronic caliper with least count of 0.01mm is used to measure the dry mandible linear dimensions (Fig. 4b). The linear dimensions were measured three times, for consistency and closest repeated value was chosen as accuracy criteria. Dimensional errors are calculated by Equation 2. These 3D CAD model dimensions and dimensional errors are shown in Table 3.

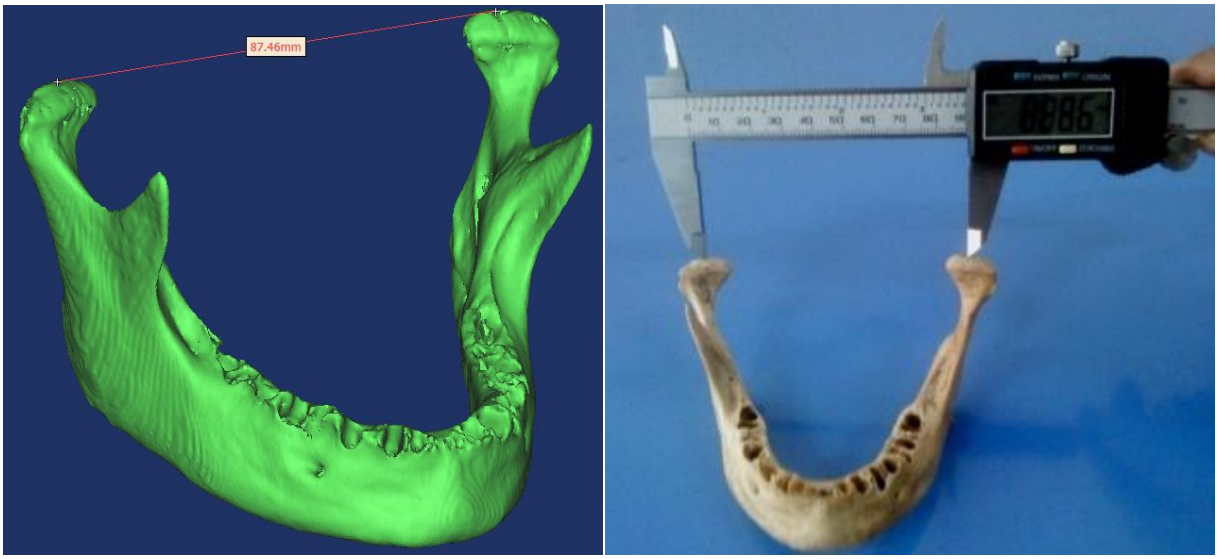

(a) (b)

Fig. 4: Dimensions are measured by (a) MIMICSsoftware and (b) digital electronic caliper

Table 3 Dimensional measurements of dry mandible and CAD models

Dimensions		X-axis Dimensions		Y-axis Dimensions		Z-axis Dimensions	
		BCoW (mm)	BCrW (mm)	PHRR (mm)	RMB (mm)	MMH (mm)	AHLR (mm)
Dry mandible		88.86	87.07	59.46	62.44	20.06	55.60
Exp. No. 1	CAD Model	87.46	85.16	58.08	61.05	19.02	54.17
	Dimensional Error	1.40	1.91	1.38	1.39	1.04	1.43
Exp. No. 2	CAD Model	87.47	85.92	58.12	60.96	19.21	54.05
	Dimensional Error	1.39	1.15	1.34	1.48	0.85	1.55
Exp. No. 3	CAD Model	87.68	85.55	58.09	61.31	19.22	54.59
	Dimensional Error	1.18	1.52	1.37	1.13	0.84	1.01
Exp. No. 4	CAD Model	87.66	85.98	58.36	61.19	19.19	54.73
	Dimensional Error	1.20	1.09	1.10	1.25	0.87	0.87
Exp. No. 5	CAD Model	88.40	86.04	58.52	60.93	19.25	55.09
	Dimensional Error	0.46	1.03	0.94	1.51	0.81	0.51
Exp. No. 6	CAD Model	88.09	85.89	58.62	61.65	19.64	54.89
	Dimensional Error	0.77	1.18	0.84	0.79	0.42	0.71
Exp. No. 7	CAD Models	87.97	86.25	58.75	61.83	19.77	54.78
	Dimensional Error	0.89	0.82	0.71	0.61	0.29	0.82
Exp. No. 8	CAD Model	88.32	86.42	58.75	61.85	19.83	54.89
	Dimensional Error	0.54	0.65	0.71	0.59	0.23	0.71
Exp. No. 9	CAD Model	88.22	86.49	58.83	61.85	19.86	55.11
	Dimensional Error	0.64	0.58	0.63	0.59	0.20	0.49

The 3D CAD mandible volumes were measured with MIMICS software. Dry mandible volume was measured by using water displacement method. In this method, the dry mandible volume is measured by calculating how much water it displaces, or pushes aside when it's placed

into distilled water. Dry mandible volume is calculated by subtracting the volume of the water without the dry mandible from the new measurement with the dry mandible. The measurements were measured in cubic millimeters (mm^3). These volumes are shown in Table 4. In this paper the difference between dry mandible volumes to the 3D CAD mandible volume values are considered as a volumetric error. This can be written as the following mathematical relations:

Volumetric error = Dry mandible volume - 3D CAD mandible volume ---------- (3)

As per Equation 3, the volumetric errors were calculated and these values are shown in Table 4.

Table 4 Volume measurement of dry mandible and CAD model

Volume taken from		Volume (mm^3)
Dry mandible		32340
Exp. No. 1	CAD Model	25547
	Volumetric Error	6793
Exp. No. 2	CAD Model	25779
	Volumetric Error	6561
Exp. No. 3	CAD Model	25969
	Volumetric Error	6371
Exp. No. 4	CAD Model	26350
	Volumetric Error	5990
Exp. No. 5	CAD Model	26592
	Volumetric Error	5748
Exp. No. 6	CAD Model	26876
	Volumetric Error	5464
Exp. No. 7	CAD Model	27460
	Volumetric Error	4880
Exp. No. 8	CAD Model	27920
	Volumetric Error	4420
Exp. No. 9	CAD Model	28448
	Volumetric Error	3892

Taguchi methods [15] have been widely utilized in engineering analysis and consist of a plan of experiments with the objective of experimentation data in a controlled way. In this work Taguchi technique was used to find the optimized parameters of tube voltage, tube current and pitch, with multiple performance characteristics of dimensional and volumetric errors. The experimental results were analyzed by analysis of variance (ANOVA) and significant main factors are identified [16]. Multiple regression equations are formulated for estimating predicted values of the dimensional and volumetric errors.

Results

In this method, the average value of the two dimensional error values was considered as an each individual axis of the dimensional error. The average value of X, Y and Z axes were considered as the overall dimensional error for each set of experimentation. The experiment was done with the default setting parameters of tube voltage 120 kV, tube current 300 mA and pitch

0.516 and resulted average dimensional and volumetric errors are 1.43 mm and 6793 mm^3 respectively, these values are shown in experiment number 1 of Table 5.

The dimensional and volumetric error of each set of L_9 orthogonal array experimentation values are depicted in Table 5. In this study smaller-the-better quality characteristic is used. The signal to noise (S/N) ratio used for this type quality characteristic is defined as [15]:

$$\frac{S}{N} = -10\log_{10}\frac{1}{n}\left(\sum_{i=0}^{i=n} y_i^2\right) \text{----------} \quad (4)$$

Where, n = number of measurements in a trial/row and y = measured value in a run/row.

Table 5 Dimensional and volumetric errors

Experiment Number	Dimensional Error (mm)				Volumetric Error (mm^3)	S/N ratio
	X-axis	Y-axis	Z-axis	Average		
Exp. No. 1	1.65	1.39	1.24	1.43	6793	-73.63
Exp. No. 2	1.27	1.41	1.20	1.29	6561	-73.33
Exp. No. 3	1.35	1.25	0.92	1.18	6371	-73.07
Exp. No. 4	1.15	1.18	0.87	1.06	5990	-72.53
Exp. No. 5	0.74	1.23	0.66	0.88	5748	-72.18
Exp. No. 6	0.97	0.82	0.57	0.78	5464	-71.73
Exp. No. 7	0.85	0.66	0.56	0.69	4880	-70.75
Exp. No. 8	0.59	0.65	0.47	0.57	4420	-69.89
Exp. No. 9	0.61	0.61	0.35	0.52	3892	-68.79

The S/N ratio values are calculated with average dimensional and volumetric errors by using Equation 4. These values are shown in last column of Table 5. Mean of S/N ratio for each level of CT image acquisition parameters were calculated. These are shown in Table 6. In order to analyses the effect of CT image acquisition parameters on the average dimensional and volumetric errors, a main effects plot for S/N ratios of optimized parameters were generated by using Minitab software, this is shown in Fig. 5. From these it was found that the optimal CT image acquisition parameters are tube voltage 80 kV, tube current 500 mA and pitch 0.984.

Table 6 Response table for S/N ratios of CT image acquisition

Parameter	Levels of Parameters			Delta	Rank
	1	2	3		
Tube voltage (kV)	-73.34	-72.15	-69.82*	3.53	1
Tube current (mA)	-72.31	-71.80	-71.20*	1.11	2
Pitch	-71.76	-71.55*	-72.00	0.45	3

*optimized level of parameters

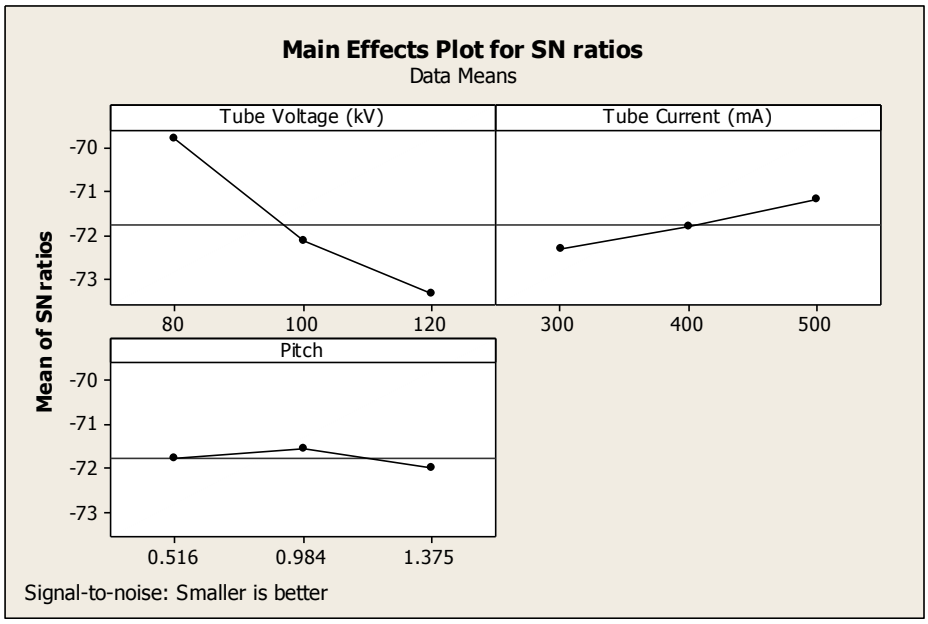

Fig. 5: Effect of process parameters on dimenstional and volumetric errors

Table 7 shows the results of ANOVA for the dimensional and volumetric errors. This analysis was carried out for a level of significance of 2%, i.e., for 98% level of confidence. The purpose of ANOVA is to investigate, which the CT image acquisition parameter significantly affects the performance characteristics. The factor of tube voltage has 91% of contribution, is the most significant control parameter for CT image acquisition stage.

Table 7 ANOVA results of the CT image acquisition parameters

Parameters	Degree of freedom	Sum of squares	Mean square	F-ratio	Percent contribution
Tube Voltage	2	1810192	905096	181.44	91%
Tube Current	2	156348	78174	15.67	7.8%
Pitch	2	12983	6491	1.30	0.7%
Error	2	9977	4988		0.5%
Total	8	1989499			100%

A multiple linear regression models are developed in order to predict the values of dimensional and volumetric errors of the medical models. The developed models are reasonably accurate and can be used for prediction within limits. The regression equations for the dimensional and volumetric errors were generated with the help of Minitab software is as:

Dimensional Error = -0.358 + 0.0177 Tube Voltage - 0.00117 Tube Current - 0.0092 Pitch---- (5)

Volumetric Error = 1305 + 54.4 Tube Voltage - 3.23 Tube Current + 115 Pitch ---------- (6)

The confirmation experiment is a crucial step and is highly recommended by Taguchi to verify the experimental results. Based on S/N ratio values, optimum process parameters were estimated by using response table and response graph as shown in Fig.5. These optimal CT image acquisition parameters are selected for the confirmation test. The default settings of

scanner parameters and optimized (confirmation experiment) parameters and its results are shown in the Table 8.

Table 8 Comparison of default scanner parameters, optimized parameters and their result

Parameter	Default parameters	Optimized parameters
Tube Voltage (kV)	120	80
Tube Current(mA)	300	500
Pitch	0.516	0.984
Average Dimensional Error (mm)	1.43	0.52
Volumetric Error (mm^3)	6793	3892

Conclusions

In this work, an attempt was made to reduce the dimensional and volumetric error of the medical models. The default settings of the scanner parameters and optimized parameters results are listed in Table 8. From the Table 8, it has been observed that the dimensional error decreased by 0.91 mm when compared with default settings. The volumetric error decreased by 2901 mm^3. Even after optimization of CT scanner small dimensional and volumetric errors do occur. The elimination of errors occurring during the CT image construction stage is also very essential because it is one of the stages of RP model fabrication.

Appendix: Linear Measurements of Mandible

Bicondylar width (BCoW) - distance between right and left uppermost point of the condyles.

Bicoronoid width (BCrW) - distance between right and left uppermost point of the coronoids.

Posterior height of right ramus (PHRR) - distance from uppermost point of the head of the condyle to lowermost and posterior point of the mandible angle, right side.

Right mandible body (RMB) - distance from lowermost and posterior point of the mandible angle to lowermost point of the middle line of the mandible symphysis, right side

Median mandible height (MMH) - distance from lowermost point of the middle line of the mandible symphysis to upper most point of the alveolar crest between the alveoli of mandibular central incisors.

Anterior height of the left ramus (AHLR) - distance from uppermost point of the coronoid process to lowermost and posterior point of the mandible angle, left side.

References

1. Pham. D. T and Gault. R. S, “A comparison of rapid prototyping technologies”, International Journal of Machine Tools & Manufacture, 1997, vol 38, P.P 1257–1287.
2. Chua. C. K and Leong. K. F. Rapid Prototyping, Principles and Applications in Manufacturing, World Scientific, 2000.
3. Gebhardt, A, Rapid Prototyping, Hanser Gardner Publications, Inc., 2003.

4. Gibson. I, Cheung. L. K, Chow S. P, Cheung. W. L, Beh. S. L, Savalani. M, Lee. S. H, "The use of rapid prototyping to assist medical applications", Assises Europeennes de Prototypage Rapide, 2004, vol 14.
5. Webb. P. A, "A review of rapid prototyping (RP) techniques in the medical and biomedical sector", 2000, vol 24, P.P 149–153.
6. Dewulf. W, Tan. Y and Kiekens. K, "Sense and non-sense of beam hardening correction in CT metrology", CIRP Annals - Manufacturing Technology, 2012, vol 61, P.P 495–498.
7. Imura. Y, Yanagida. T, Morii. H, Mimura. H, Aoki. T, "Reduction of the Beam Hardening Artifacts in the X-Ray Computer Tomography: Energy Discrimination with a Photon-Counting Detector", World Journal of Nuclear Science and Technology, 2012, vol 2, P.P 169–173.
8. Maa. C, Baer and Kachelrie. M, "Image-based dual energy CT using optimized pre correction functions: A practical new approach of material decomposition in image domain", International Journal of Medical Physic Research and Practice, 2009, vol36, P.P 3818–3829.
9. Schindera. T. S, Marin. I. T. D, Nelson. R. C, Raupach. R, Hagemeister. M, Allmen. G, Vock. P, Farkas. Z. S, "Effect of Beam Hardening on Arterial Enhancement in Thoracoabdominal CT Angiography with Increasing Patient Size: An in Vitro and in Vivo Study", Journal of Radiology, 2010, vol 256, P.P 528–535.
10. Tanaka. C, Ueguchi. T, Shimosegawa. E, Sasaki. N, Johkoh. T, Nakamura. H, Hatazawa. J, "Effect of CT Acquisition Parameters in the Detection of Subtle Hypoattenuation in Acute Cerebral Infarction: A Phantom Study", American Journal of Neuroradiology, 2006, vol 27, P.P 40–45.
11. Bisogni. M. G, Guerra. A. D, Lanconelli. N, Lauria. A, Mettivier. G, Montesi. M. C, Panetta. D, Pani. R, Quattrocchi. M. G, Randaccio. P, Rosso. V, Russo. P, "Experimental study of Beam Hardening artifacts in photon counting breast computed tomography", International Journal of Nuclear Instruments and Methods in Physics Research, 2007, vol 581, P.P 94–98.
12. Zhang. Y, Mou. X and Tang. S, "Beam Hardening Correction for Fan-beam CT Imaging with Multiple Materials", IEEE Transactions on Nuclear Science Symposium Conference Record (NSS/MIC), 2010, P.P 3566 – 3570.
13. Light Speed™ VCT Technical Reference Manual, General Electric Company, 2011.
14. Materialise NV, Technologielaan 15, 3001 Leuven, Belgium. (www.materialise.com/mimics)
15. Taguchi G, Introduction to quality engineering, Asian Productivity Organization, 1990.
16. Sharma N, Ahmad S, Khan Z. A, Siddiquee A. N, "Optimization of cutting parameters for surface roughness in turning". International journal of Advanced research in engineering and technology, 2012,vol 3, P.P 86-96.